COMPARATIVE ANALYSIS OF HYBRID COMPOSITES BASED ON A356 AND ZA-27 ALLOYS REGARDING THEIR TRIBOLOGICAL BEHAVIOUR

Blaža Stojanović[1], Sandra Gajević[1,*], Nenad Miloradović[1], Ružica Nikolić[2], Slavica Miladinović[1], Petr Svoboda[3], Aleksandar Vencl[4]

[1]University of Kragujevac, Faculty of Engineering, Kragujevac, Serbia
[2]Research Centre, University of Zilina, Zilina, Slovakia
[3]Faculty of Mechanical Engineering, Brno University of Technology, Brno, Czechia
[4]University of Belgrade, Faculty of Mechanical Engineering, Belgrade, Serbia

*E-mail of corresponding author: sandrav@kg.ac.rs

Blaža Stojanović 0000-0003-4790-2856,
Nenad Miloradović 0000-0001-6846-6091,
Slavica Miladinović 0000-0002-4408-0634,
Aleksandar Vencl 0000-0002-2208-4255
Sandra Gajević 0000-0002-7169-8907,
Ružica Nikolić 0000-0003-3042-8916,
Petr Svoboda 000-0003-3091-4025,

Resume

The comparative analysis of the two hybrid composites, obtained by the compocasting process, based on A356 and ZA-27 alloys and reinforced with 10 wt. % SiC and 0, 1 and 3 wt. % graphite (Gr) is presented. Optimisation of their tribological behaviour was performed by the Taguchi method and the artificial neural network (ANN). Tribological tests were performed on a block-on-disk tribometer, at three sliding speeds, three normal loads and a sliding distance of 600 m, without lubrication. Results obtained by the ANOVA showed that the hybrid composites based on A356 alloy have the better wear resistance and that the composite reinforced with 10 wt. % SiC and 1 wt. % Gr has the lowest wear rate. The lowest coefficient of friction was obtained for a composite based on ZA-27 alloy reinforced with 10 wt. % SiC, at a normal load of 10 N and sliding speed of 1 m/s.

Article info

Received 25 April 2023
Accepted 19 June 2023
Online 27 June 2023

Keywords:

wear
hybrid composites
A356
ZA-27
Taguchi design
artificial neural network

Available online: https://doi.org/10.26552/com.C.2023.056

ISSN 1335-4205 (print version)
ISSN 2585-7878 (online version)

1 Introduction

Requirements of the modern society, from the aspect of the service life increase and reduction of mass and thus the construction prices, initiated development of the new composites based on light metals. Composite materials could be made with metal, ceramic or polymer matrix and contain two or more physically distinct and mechanically separable materials [1]. Out of all the metal matrix composites (MMCs), the largest share in the world production belongs to composite materials based on aluminium alloys – over 30 % of the total production of composite materials. This market share is primarily due to the large use of MMCs with an aluminium matrix in aerospace, automotive, electronics and military industries. With an annual growth rate of 6 – 7 %, composite materials with a metal matrix are very interesting and promising materials. Hybrid composites are composites with two or more types or shapes of reinforcements.

Sardar et al. [2] have modelled the tribological characteristics of Al-Zn-Mg-Cu matrix composites with help of artificial neural network (ANN) and genetic algorithm (GA) methodology. They varied the amount of the Al_2O_3 particles (0 - 20 wt. %), load (20 - 80 N), abrasive size (9 - 105 μm) and sliding speed (0.125 - 1.50 m/s). The ANN and GA were used to reduce the wear rate, coefficient of friction and roughness of the abraded surface. The lowest wear rate and coefficient of friction were for 15 ± 2 wt. % of particles amount in the composite, while roughness was lower for particle amount in the range from 10 to 20 wt. %. At confirmation of experiments, the error results were lower than, or equal to, 12 %, which indicates the good

applicability of the developed model. It has been shown that the simultaneous use of ANN and GA leads to reliable results, which can be obtained in a relatively short period.

Nwobi-Okoye et al. [3] performed modelling and multi-objective optimisation of age hardening process parameters of composites based on A356 alloy, using the ANN and adaptive neuro-fuzzy inference system (ANFIS). By data analysis, it was concluded that the ANN with coarse experimental data points for learning is more effective than the ANFIS in predicting the process outputs. Ekka et al. [4] applied the regression analysis and the ANN method to predict the wear rate and coefficient of friction of hybrid composites. They came to a similar conclusion by analysing the experimental data – it was found that the ANN is more efficient in predicting the wear rate than the regression analysis.

Güler et al. [5, 6], considered the effect of content of the nano graphite particles on the wear behaviour of ZA27 based hybrid composites and nano composite bearing materials with enhanced corrosion properties. The lowest wear loss was obtained for the hybrid nanocomposites with content of 4 vol. % of graphite and 4 vol. % of alumina. The abrasion was the dominant wear mechanism in all the hybrid nanocomposites except for the mentioned one, where the adhesion was the dominant wear mechanism. For the nanocomposites obtained by mechanical milling, followed by hot pressing, authors reported that an increase of the milling duration improved the corrosion resistance of the nanocomposite bearing materials.

Celebi et al. [7], studied the effect of the nanoparticle content on the microstructure and mechanical properties of the ZA27 based hybrid composites produced by the powder metallurgy. Due to the lubricating properties of Gr, the negative effect of the mechanical-milling process caused the composite powder size to increase with cold-welding and to take a flaky shape. As the n-Gr ratio increased, cold-welding and agglomeration of additives during the mechanical milling increased the amount of porosity, while the tensile strength and hardness values of (hybrid nano composite materials) HNMs decreased as the n-Gr ratio increased, an increase was achieved with the increase in the n-Al_2O_3 ratio.

Feng, Wang and Wang [8], analysed the influence of graphite morphology on hyperthermal friction and wear behaviours of aluminium alloys with high silicon content. The volumetric wear loss results denote that (Al-27Si)-5FG (fake graphite) composites possess the superior wear resistance with respect to the Al-27Si and (Al-27Si)-5PG (particle graphite) composites for all the test temperatures. Due to the weak bonding of graphite particles, (Al-27Si)-5PG has the biggest volume wear. When the temperature rises to 400 °C, coefficient of friction of all the samples had a big fluctuations because of aluminium matrix softening and vibrations.

Ashebir et al. [9], reviewed the mechanical and metallurgical behaviour of hybrid reinforced aluminium metal matrix composites, various production methods, as well as the effect of various reinforcement ceramic particles and graphite (Gr) on the mechanical and metallurgical properties of MMCs. They pointed that the graphite, used as a solid lubricant between the composite material and the counter-body significantly lowered the composite wear, without the requirement of lubrication.

The microstructural, mechanical and tribological behaviour of aluminium-silicon A356 alloy and zinc-aluminium ZA-27 alloy hybrid metal matrix composites, is presented in [10-14]. Many authors have found that optimisation methods, such as Taguchi, GA, particle swarm optimisation (PSO) and others, can be successfully used when optimising the production parameters [15-16], processing or composition of composites [17-20], but that the better results are obtained by training or using the ANN. In this paper, the tribological behaviour of composites with the addition of graphite as a second reinforcement is optimised with the use of the Taguchi method and ANN. The matrices used for production of hybrid composites were A356 and ZA-27 alloys.

2 Experimental procedures

2.1 Materials and manufacturing

Two different matrices were used in production of the composites: the A356 alloy and ZA-27 alloy, reinforced with 10 wt. % SiC, the average size of 40 μm. Graphite (Gr) was also added to the composites. The average Gr particles size was 35 μm, while the amount of Gr particles varied and was 1 and 3 wt. %. Hybrid composites were obtained by applying the compocasting process. A detailed description of the process of obtaining the hybrid composites with the A356 base can be found in [21] and for the composites with the ZA-27 base in [18]. Structures of investigated composites (A356+10SiC and ZA-27+10SiC) and hybrid composites (A356+10SiC+1Gr, A356+10SiC+3Gr, ZA-27+10SiC+1Gr, ZA-27+10SiC+3Gr) are shown in Figure 1. It can be noticed that the SiC particles distribution is favourable and that the area of the matrix without particles is reduced. The soft Gr particles did not retain their average size during the composite production process. They were eroded and crushed in the process of preparation, so their final size was much smaller than the starting one.

Before examining the tribological characteristics, the hardness of the obtained composites was measured. The hardness of the tested materials was measured according to Vickers method (load of 10 kg) and the measurements were repeated 3 times and the mean values are presented in Table 1.

It was observed that the addition of a larger amount

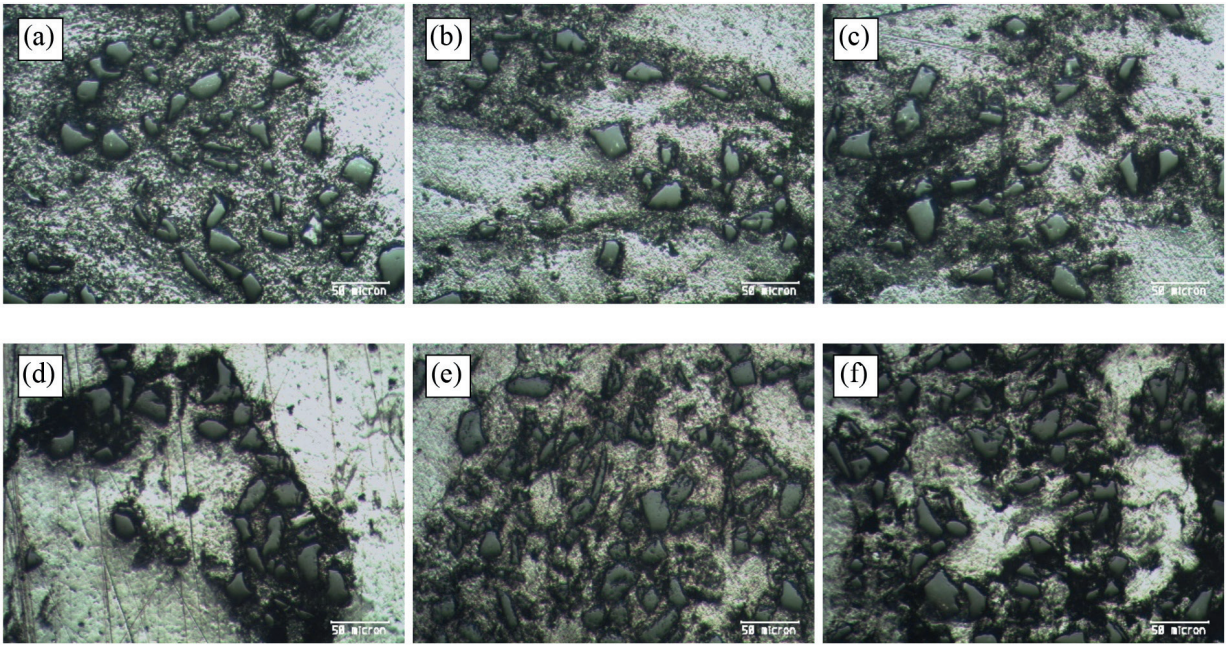

Figure 1 *Structures of the tested composites: (a) A356+10SiC, (b) A356+10SiC+1Gr, (c) A356+10SiC+3Gr, (d) ZA-27+10SiC, (e) ZA-27+10SiC+1Gr and (f) ZA-27+10SiC+3Gr*

Table 1. *Hardness of the tested composites*

Test no.	Material	HV
1	A356+10 wt.%SiC	68
2	A356+10 wt.% SiC+1 wt.% Gr	60
3	A356+10 wt.% SiC+3 wt.% Gr	46
4	ZA-27+10 wt.% SiC	125
5	ZA-27+10 wt.% SiC+1 wt.% Gr	127
6	ZA-27+10 wt.% SiC + 3 wt.% Gr	114

of graphite (3 wt.%) leads to a decrease in hardness for both hybrid composites. It is evident that the measured hardness values are correlated with the wear of the composite.

2.2 Wear and friction tests

The wear and friction tests of hybrid composites with different matrices were performed in dry sliding conditions, on a tribometer with the block-on-disc contact geometry. The material of the disc was a MANCOVA steel of hardness of 62-64 HMRC and a diameter of 35 mm and thickness of 6.35 mm, while the block materials were made of tested hybrid composites. The geometry of the contact pairs was in accordance with the standard ASTM G77. Values of the coefficient of friction (COF) were monitored during the test and through the data acquisition system stored in the PC. The wear rate used in the further analysis was obtained by calculations based on the wear scar width, which was measured on a universal measuring microscope, after 600 m of sliding distance. All the tribological tests were repeated 3 times and mean values are shown in the wear rate results.

2.3 Experimental design

The modern approach to experiments is closely connected with the use of the experiments' design. Experimental planning is a powerful tool for experimental statistical research of complex systems. Its application provides a practical and efficient way of varying the influential or input factors at different levels, contributing to an objective understanding of the researched system/process with help of statistics. The experimental design methodology is a systematic way to plan, perform and interpret the results of experiments, to obtain as much information as possible, while performing as few experiments as possible [22].

Realisation of the experimental test in this research was performed according to the defined plan, which consisted of selected factors and their levels given in Table 2. The sliding distance for all the tests was kept

Table 2 *Levels for various control factors*

Control factor	Units	Level I	Level II	Level III
(A) Material	-	A356+10SiC	ZA-27+SiC	-
(B) Gr amount	wt.%	0	1	3
(C) Normal load	N	10	20	30
(D) Sliding speed	m/s	0.25	0.50	1.0

Table 3 *Experimental design using L54 orthogonal array and wear and friction test results*

Test no.	A	B	C	D	Wear rate $\times 10^{-3}$, mm^3/m	S/N ratio for wear rate	COF	S/N ratio for COF
1	A356+10SiC	0	10	0.25	0.367	8.7067	0.703	3.06089
2	A356+10SiC	0	20	0.25	1.548	-3.7954	0.690	3.22302
3	A356+10SiC	0	30	0.25	1.846	-5.3246	0.650	3.74173
4	A356+10SiC	0	10	0.50	0.687	3.2609	0.689	3.23562
5	A356+10SiC	0	20	0.50	1.768	-4.9496	0.655	3.67517
6	A356+10SiC	0	30	0.50	2.119	-6.5226	0.621	4.13817
7	A356+10SiC	0	10	1.00	0.869	1.2196	0.640	3.87640
8	A356+10SiC	0	20	1.00	2.144	-6.6245	0.623	4.11024
9	A356+10SiC	0	30	1.00	2.310	-7.2722	0.579	4.74643
10	A356+10SiC	1	10	0.25	0.135	17.3933	0.724	2.80523
11	A356+10SiC	1	20	0.25	0.696	3.1478	0.710	2.97483
12	A356+10SiC	1	30	0.25	1.687	-4.5423	0.680	3.34982
13	A356+10SiC	1	10	0.50	0.197	14.1107	0.694	3.17281
14	A356+10SiC	1	20	0.50	0.909	0.8287	0.677	3.38823
15	A356+10SiC	1	30	0.50	1.833	-5.2632	0.660	3.60912
16	A356+10SiC	1	10	1.00	0.282	10.9950	0.657	3.64869
17	A356+10SiC	1	20	1.00	1.253	-1.9590	0.652	3.71505
18	A356+10SiC	1	30	1.00	2.085	-6.3821	0.646	3.79535
19	A356+10SiC	3	10	0.25	0.173	15.2391	0.733	2.69792
20	A356+10SiC	3	20	0.25	1.372	-2.7471	0.743	2.58022
21	A356+10SiC	3	30	0.25	2.306	-7.2572	0.824	1.68146
22	A356+10SiC	3	10	0.50	0.244	12.2522	0.712	2.95040
23	A356+10SiC	3	20	0.50	1.580	-3.9731	0.717	2.88962
24	A356+10SiC	3	30	0.50	2.532	-8.0693	0.771	2.25891

constant at 600 m. The varied factors were different composite matrices, amount of composite reinforcements, normal load and sliding speed.

Based on the defined factors and the adopted levels, the Taguchi orthogonal array L54 was obtained with Minitab 16. The experimental results are shown in Table 3, as well as the values of the S/N (signal-to-noise) ratios obtained by the data analysis. In the Taguchi method, the transformation of experimental results into the S/N relationships is mandatory. There are three categories of the S/N relationships: "smaller-is-better", "larger-is-better" and "nominal-is-best". In this case, the quality characteristic S/N ratio "smaller-is-better" was selected for the analysis of the composite wear rate [14]. Statistical analysis of variance is used to consider statistically worthy parameters so that the optimal combination of parameters can be predicted.

3 Results and discussion

3.1 Wear rate and coefficient of friction

Depending on the purpose of the output, the appropriate characteristics was chosen. However, regardless of the selected output category, the higher S/N ratio corresponds to the better-quality characteristics and, more precisely, to the smaller variance of the output characteristics (response) around the desired (target) value. The arithmetic mean of the S/N ratio was calculated for each level of the considered factors in comparison to the wear rate (Table 4).

Based on the results of the S/N ratios (Table 4 and Figures 2 and 3), it can be determined which of the considered factors has the greatest influence on the wear rate. In addition, an optimal combination of

Table 3 *(continued) Experimental design using L54 orthogonal array and wear and friction test results*

Test no.	A	B	C	D	Wear rate $\times 10^{-3}$, mm³/m	S/N ratio for wear rate	COF	S/N ratio for COF
25	A356+10SiC	3	10	1.00	0.346	9.2185	0.690	3.22302
26	A356+10SiC	3	20	1.00	1.894	-5.5476	0.708	2.99933
27	A356+10SiC	3	30	1.00	2.952	-9.4023	0.750	2.49877
28	ZA-27+10SiC	0	10	0.25	0.512	5.8146	0.486	6.26549
29	ZA-27+10SiC	0	20	0.25	2.237	-6.9933	0.513	5.79088
30	ZA-27+10SiC	0	30	0.25	2.441	-7.7514	0.538	5.38758
31	ZA-27+10SiC	0	10	0.50	0.531	5.4981	0.513	5.80104
32	ZA-27+10SiC	0	20	0.50	2.288	-7.1891	0.532	5.47524
33	ZA-27+10SiC	0	30	0.50	2.606	-8.3195	0.553	5.13765
34	ZA-27+10SiC	0	10	1.00	0.592	4.5536	0.527	5.56214
35	ZA-27+10SiC	0	20	1.00	2.402	-7.6115	0.552	5.16279
36	ZA-27+10SiC	0	30	1.00	2.703	-8.6369	0.583	4.68514
37	ZA-27+10SiC	1	10	0.25	0.365	8.7541	0.483	6.31926
38	ZA-27+10SiC	1	20	0.25	2.002	-6.0293	0.497	6.07462
39	ZA-27+10SiC	1	30	0.25	2.258	-7.0745	0.517	5.73187
40	ZA-27+10SiC	1	10	0.50	0.422	7.4938	0.497	6.07112
41	ZA-27+10SiC	1	20	0.50	2.206	-6.8721	0.505	5.94106
42	ZA-27+10SiC	1	30	0.50	2.339	-7.3806	0.530	5.51940
43	ZA-27+10SiC	1	10	1.00	0.512	5.8146	0.511	5.83328
44	ZA-27+10SiC	1	20	1.00	2.245	-7.0243	0.535	5.43942
45	ZA-27+10SiC	1	30	1.00	2.401	-7.6078	0.540	5.34891
46	ZA-27+10SiC	3	10	0.25	0.252	11.9720	0.500	6.01713
47	ZA-27+10SiC	3	20	0.25	2.033	-6.1627	0.516	5.74869
48	ZA-27+10SiC	3	30	0.25	2.231	-6.9700	0.532	5.48013
49	ZA-27+10SiC	3	10	0.50	0.384	8.3134	0.516	5.75206
50	ZA-27+10SiC	3	20	0.50	2.051	-6.2393	0.532	5.48013
51	ZA-27+10SiC	3	30	0.50	2.288	-7.1891	0.547	5.24184
52	ZA-27+10SiC	3	10	1.00	0.451	6.9165	0.539	5.36500
53	ZA-27+10SiC	3	20	1.00	2.091	-6.4071	0.556	5.09694
54	ZA-27+10SiC	3	30	1.00	2.358	-7.4509	0.568	4.91762

Table 4 *Response table for signal-to-noise ratios for wear rate and COF*

Level	Wear rate				COF			
	Material	Gr amount, %	Normal load, N	Sliding speed, m/s	Material	Gr amount, %	Normal load, N	Sliding speed, m/s
1	0.2496	-2.8854	8.7515	0.3544	3.261	4.615	4.537	4.385
2	-2.3622	0.4668	-4.7860	-1.1228	5.579	4.597	4.431	4.430
3		-0.7502	-7.1343	-2.4005		4.049	4.293	4.446
Delta	2.6118	3.3522	15.8857	2.7549	2.319	0.566	0.244	0.061
Rank	4	2	1	3	1	2	3	4

factors can be determined to achieve the minimal wear of hybrid composites. Based on Table 4 and according to the ranking of factors, it was determined that the greatest influence has the normal load, followed by other factors in this order: Gr amount, sliding speed and material. Main effects plots (Figures 2a and 3a) show that composites based on A356 alloy had lower wear and higher friction than the composites based on ZA-27 alloy. This is most probably because the SiC reinforcements protruded more to the surface of the A356 alloy thus protecting the matrix and inducing the higher friction [10]. As expected, the higher load and speed induced higher wear rates, while load and speed had a low impact on the COF values.

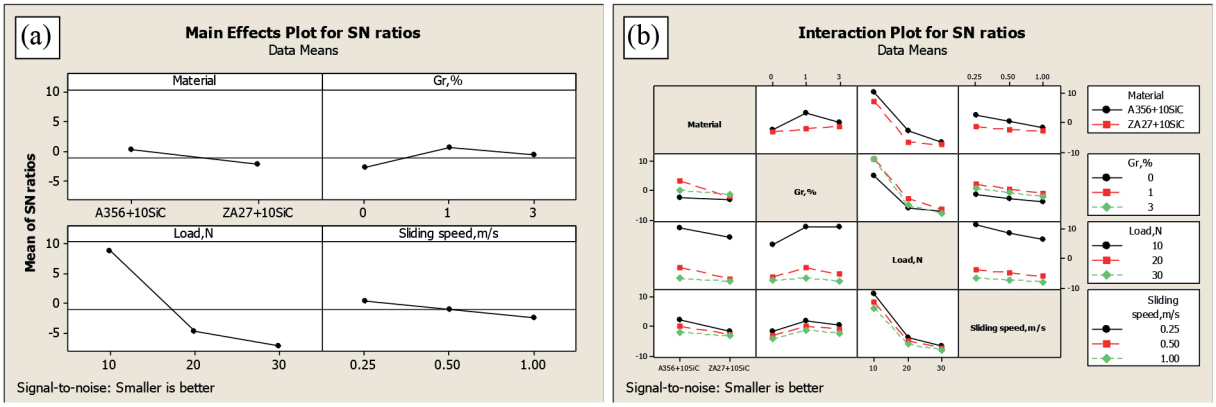

Figure 2 *The S/N ratio for the wear rate: (a) main effects plot and (b) interaction plot*

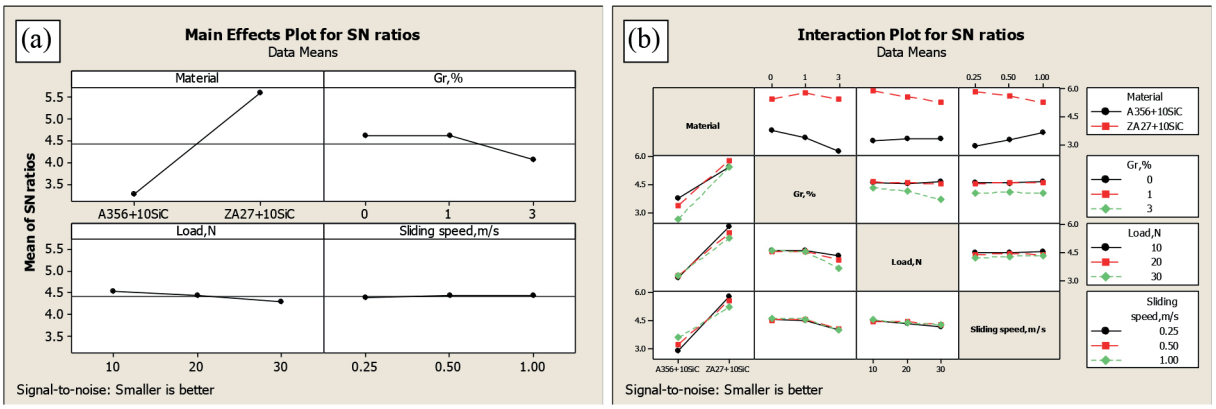

Figure 3 *The S/N ratio for the coefficient of friction: (a) main effects plot and (b) interaction plot*

The optimal combination of factors for achieving the minimum wear rate is A1-B2-C1-D1, i.e. using the composites based on aluminium alloy, A356/10 wt. % SiC with reinforcement content of 1 wt. % Gr, at a normal load of 10 N and sliding speed of 0.25 m/s. For the minimum COF, the optimal combination of factors is A2-B1-C1-D3, i.e. using the composites based on zinc alloy, ZA-27/10 wt. % SiC, with reinforcement content of 0 wt. % Gr, at a normal load of 10 N and sliding speed of 1 m/s. Figures 2b and 3b show graphs of factor interactions, according to which the existence of influence of interactions between individual factors on the wear rate is observed.

A more precise determination of the influence of factors and their interactions on the wear rate and COF of composites was performed using analysis of variance (ANOVA). With help of the ANOVA analysis, the values of members, which define the statistically significant members that represent input variables (factors), whose change affects the change of the output variable (wear rate), are obtained. The ANOVA analysis was applied at the significance level of 5 % (i.e. 95 % confidence level). The level of significance was defined by the p-value, which indicates the member's influence on the wear rate. If the calculated p-value is less than 0.05 that member affects wear, while members with a p-value greater than 0.10 should be omitted from further analysis because that indicates that they do not affect the output.

Following the results obtained by the ANOVA analysis, a large influence of normal load on the wear rate of hybrid composites of 84.53 % was observed in the last column of Table 5. It was followed by the influence of the graphite amount (3.31 %), the influence of the matrix material of the composite (2.94 %) and the influence of the sliding speed (2.19 %), while the influence of interactions was less than 3 %. Observing the results of ANOVA analysis for the COF (Table 6), a large influence of the composite matrix of 82.89 % is observed, followed by the influence of the Gr amount of 4.26 %, while the influence of the normal load and sliding speed is less than 1 %. Influence of factor interactions on the COF of 3.17 % and 4.50 % corresponds to material × Gr amount and material × sliding speed, respectively.

Figure 4 shows the contour plots of the influencing factors on the wear rate (wear maps). Based on the diagram, minimal wear was achieved by tracking the lighter colours. By adjusting the factors to certain values, it is possible to achieve the target value of the wear rate.

The wear rate increases with the load increase, while the addition of Gr particles up to 1.5 wt. % decreases the wear. Further adding of the Gr particles, above 1.5 wt. %, starts to increase the wear rate. The effect of the reinforcement in the composite is prominent at the higher applied load of around 25 N. It was noticed that the small amount of Gr particles, up to around 0.5 wt. %, at the lowest load, does not affect improving

Table 5 *Analysis of variance for the S/N ratios for wear rate*

Source	DF	Seq SS	Adj SS	Adj MS	F-value	p-value	Pr, %
Material	1	92.09	92.09	92.09	66.74	0.000	2.94
Gr amount	2	103.67	103.67	51.83	37.56	0.000	3.31
Normal load	2	2646.81	2646.81	1323.40	959.05	0.000	84.53
Sliding speed	2	68.43	68.43	34.21	24.79	0.000	2.19
Material × Gr amount	2	51.40	51.40	25.70	18.62	0.000	1.64
Material × normal load	2	20.78	20.78	10.39	7.53	0.002	0.66
Material × sliding speed	2	15.42	15.42	7.71	5.59	0.009	0.49
Gr amount × normal load	4	71.91	71.91	17.98	13.03	0.000	2.30
Gr amount × sliding speed	4	0.46	0.46	0.12	0.08	0.987	0.01
Normal load × sliding speed	4	21.42	21.42	5.36	3.88	0.012	0.68
Residual error	28	38.64	38.64	1.38			1.23
Total	53	3131.03					100.00

S = 1.175, R^2 = 98.8 %, R^2 (adj) = 97.7 %

Table 6 *Analysis of variance for the S/N ratios for COF*

Source	DF	Seq SS	Adj SS	Adj MS	F-value	p-value	Pr, %
Material	1	72.5696	72.5696	72.5696	1151.29	0.000	82.89
Gr amount	2	3.7274	3.7274	1.8637	29.57	0.000	4.26
Normal load	2	0.5381	0.5381	0.2691	4.27	0.024	0.61
Sliding speed	2	0.0357	0.0357	0.0179	0.28	0.755	0.04
Material × Gr amount	2	2.7760	2.7760	1.3880	22.02	0.000	3.17
Material × normal load	2	1.2452	1.2452	0.6226	9.88	0.001	1.42
Material × sliding speed	2	3.9399	3.9399	1.9700	31.25	0.000	4.50
Gr amount × normal load	4	0.8471	0.8471	0.2118	3.36	0.023	0.97
Gr amount × sliding speed	4	0.0624	0.0624	0.0156	0.25	0.909	0.07
Normal load × sliding speed	4	0.0440	0.0440	0.0110	0.17	0.950	0.05
Residual error	28	1.7649	1.7649	0.0630			2.02
Total	53	87.5504					100.00

S = 0.2511, R^2 = 98.0 %, R^2 (adj) = 96.2 %

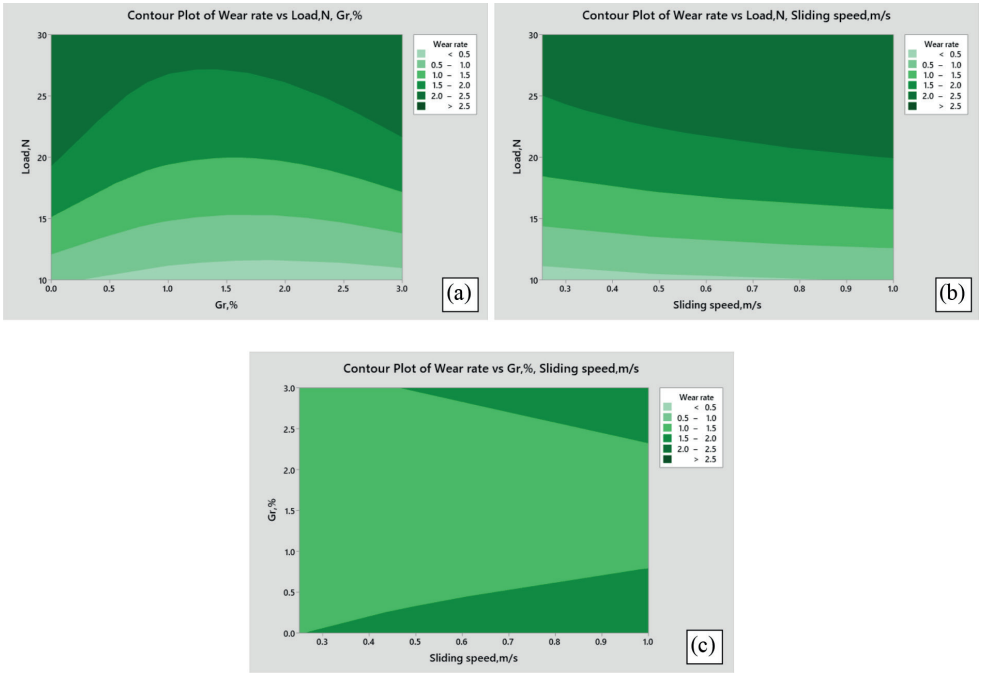

Figure 4 *Diagram of the wear rate dependence on: (a) normal load and reinforcement content, (b) normal load and sliding speed and (c) reinforcement content and sliding speed*

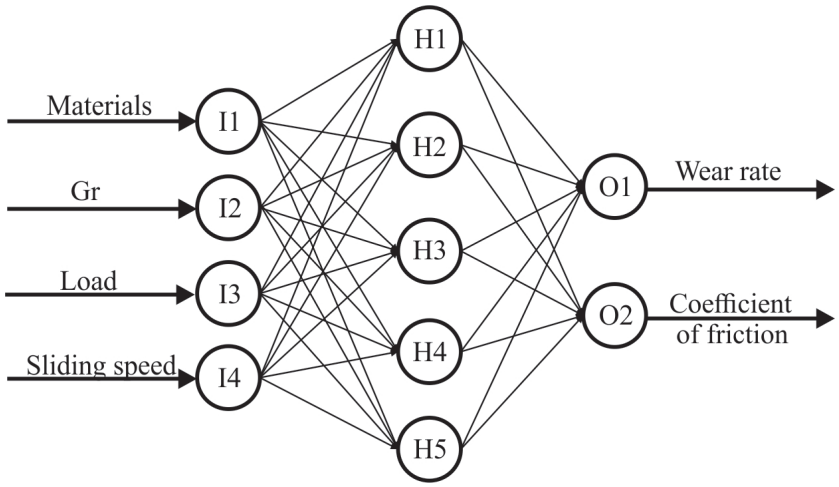

Figure 5 *The ANN architecture*

the wear resistance. The influence of the Gr particles amount on the composite wear, regarding the sliding speed, is manifested at higher sliding speeds.

3.2 The ANN prediction

The principle of solving problems using neural networks is similar to that of the human brain. Like the human brain, neural networks are made up of simple interconnected units called nodes or neurons. Neural networks are not programmed, but they learn from experience through the recognition of patterns and the interrelationship between data, so it is not important for them to know the theory behind the phenomenon. The data, based on which the network is trained, come to the input layer, then they are transferred to the hidden layer and, finally, the predicted data is obtained via the output layer [2,19]. The number of input parameters means the number of neurons in the input layer, the number of output parameters means how many neurons there are in the output layer, while the number of neurons in the hidden layer is not precisely defined and depends on the experience of a person who is modelling the network.

In the used ANN, the signals were transmitted from the input to the output, with feed-forward back propagation neural network. The Levenberg-Marquardt network training function was used in the formation and training of the network because it is recommended due to its accuracy and speed. In the hidden layer, the neurons work based on the Log-Sigmoid transfer function (logsig) and in the output layer - based on the Linear Transfer Function (purelin). In the input layer, some parameters are varied. In this case, there are four parameters: material, amount of graphite, normal load and sliding speed. Results of the experiment, i.e. the wear rate and COF are in the output layer. Several networks, with different numbers of neurons in the hidden layer (5, 10 and 15), were trained, but the network with 5 neurons in the hidden layer proved to be the best. The used network scheme was with the 4-5-2 architecture (Figure 5).

After the network training, in addition to the predicted data, the regression diagrams for training, validation, testing and the total regression coefficient were obtained (Figure 6). When developing each network, the total regression coefficient tends to be as close to 1 as possible. After training the network with the 4-5-2 architecture, the regression coefficient of 0.99456 was obtained, which shows a very good correlation with the experimental data. From Figure 6, it can be observed that the majority of the input data to the neural network were used for training (as much as 60 %), while 20 % was used for validation and 20 % for testing the developed neural network.

3.3 Wear mechanisms

The worn surfaces of the blocks were imaged on an SEM microscope and representative wear scars are shown in Figure 7. The EDS analysis of the chemical composition of individual samples was performed, as well. Before analysing the samples, they were cleaned and degreased with petrol in the ultrasonic bath. Such a sample preparation was performed to prevent contamination of the microscope, as well as to obtain a realistic picture of the condition of the worn surfaces. Appearances of all the composite samples worn surfaces were similar, regardless of the normal load and sliding speed. From Figure 7 one can see that the main wear mechanism was the adhesive wear [12]. Adhesive wear pits of irregular shape and uneven depth are visible on the worn surface of the blocks, together with the protruded SiC particles and transferred disc (counter-body) material. Regarding the counter-body sliding direction, it can be noticed that the transfer of the material occurs mainly in the first half of the wear scar and the adhesive wear pits appear mainly in the second half of the wear scar.

The SEM images and EDS analysis of the composites' samples show the presence of iron (Fe), oxygen (O), silicon (Si) and carbon (C), Figure 8. The

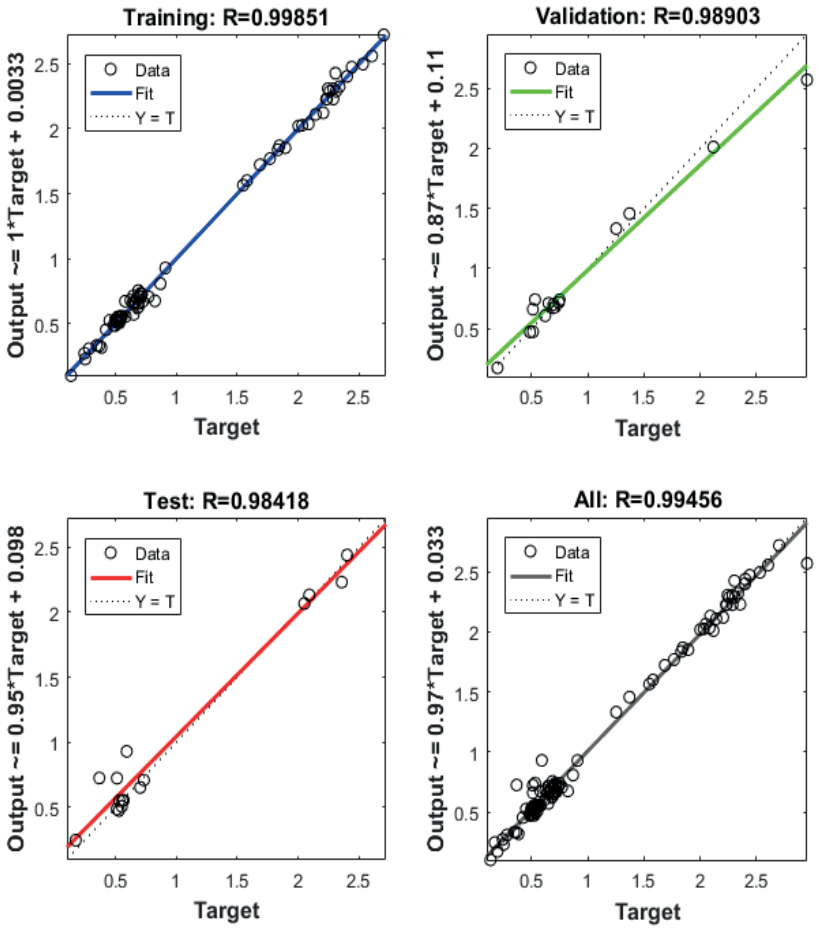

Figure 6 *Regression coefficients of the trained network*

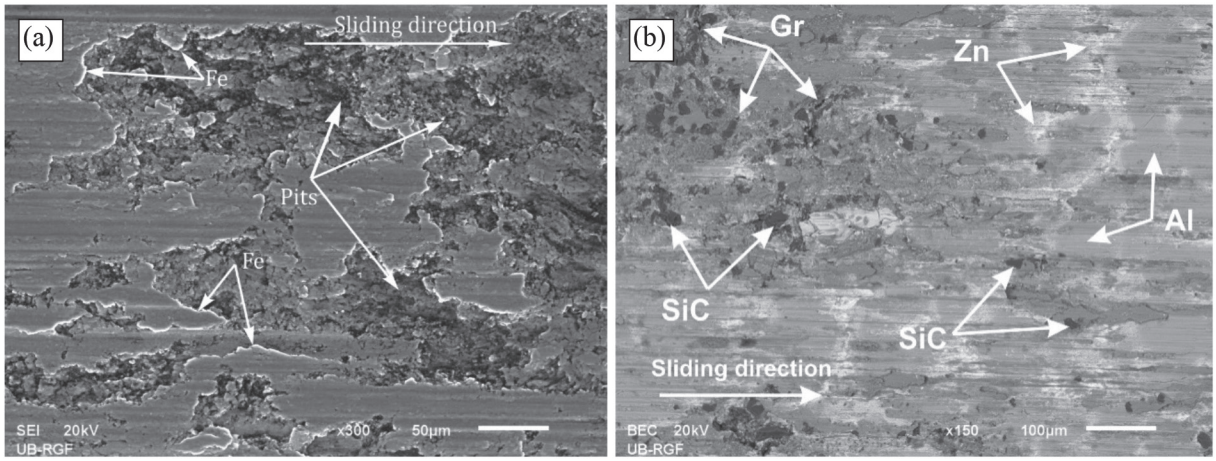

Figure 7 *The SEM image of the worn surfaces for a normal load of 10 N and sliding speed of 0.25 m/s: (a) A356+10SiC+1Gr and (b) ZA-27+10SiC+1Gr*

presence of Fe (Spectrum 2) indicates that the surface layer of the steel disc was also worn and that transfer of counter-body material occurred. The wear of the steel disc is mainly caused by the presence of the protruded SiC hard particles (Spectrum 3). The oxidized worn iron particles and matrix material formed a mechanically mixed layer (MML) [23-24], which was confirmed by the EDS analysis (Spectrum 1).

4 Conclusions

The Taguchi design and ANN can be successfully used to analyse the parameters influencing the wear rate and coefficient of friction of the tested hybrid composites. Application of the Taguchi method reduces the number of conducted experiments and the time of their realisation, as well as the costs. The ANOVA

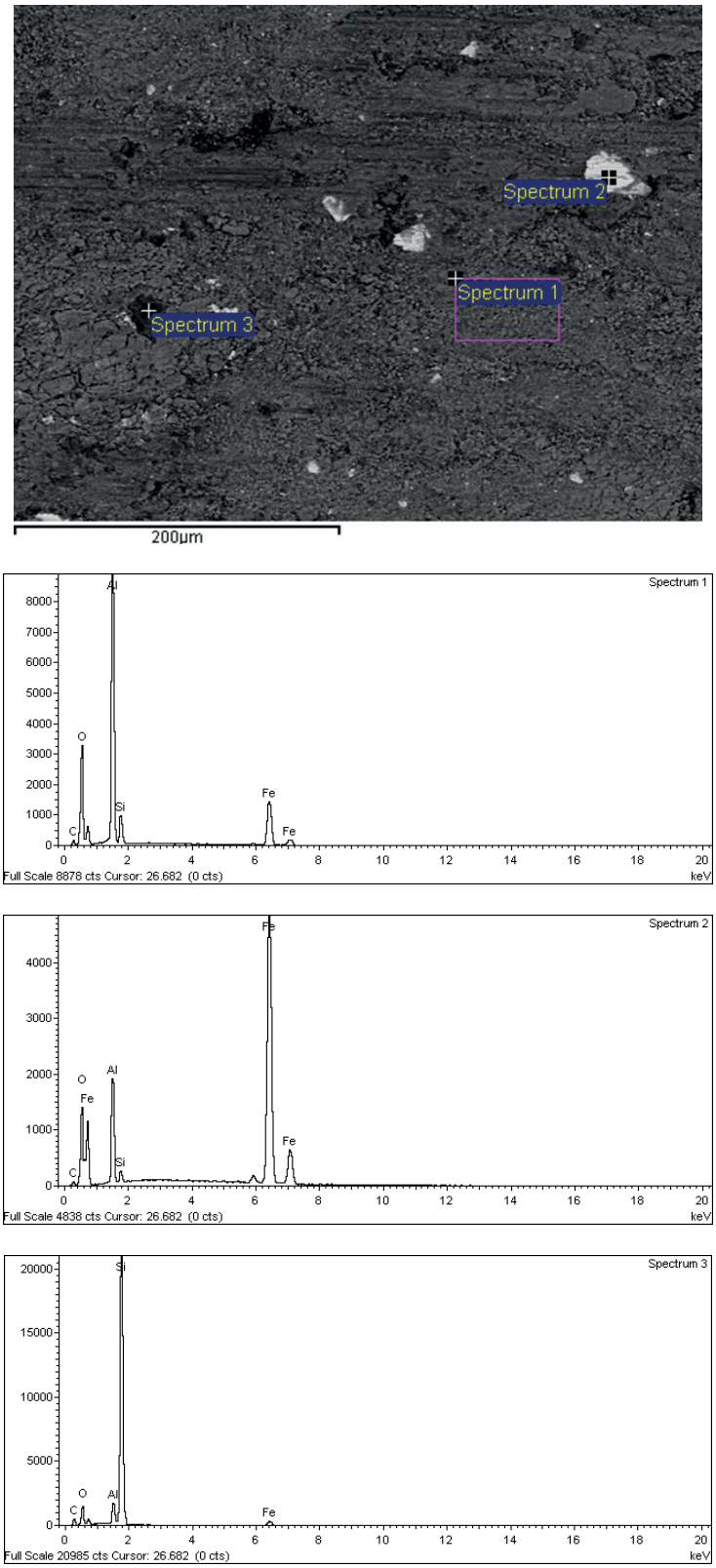

Figure 8 *The EDS analysis of hybrid composite A356+10SiC+1Gr at the normal load of 10 N and the sliding speed of 0.25 m/s*

analysis of influential parameters very precisely shows the influence of individual parameters. Based on the obtained results, it is possible to predict the wear rate and coefficient of friction, as well as to determine the values of the influential parameters that give the minimum values. An artificial neural network is used to verify the obtained results. Matching the results, using the Taguchi method and the ANN, confirmed the

justification of the application of these methods.

Based on the obtained results, it can be concluded that both hybrid composites have better characteristics than the corresponding matrix alloys. For the given test conditions, the wear of hybrid composites based on A356 alloy is lower than the wear of hybrid composites based on ZA-27 alloy, while for the coefficient of friction, it is the opposite. The dominant mechanism is adhesive wear, which is manifested through delamination and transfer of materials between the contact surfaces. Formation of the MML layers was observed in both types of composites (with aluminium alloy matrix and zinc alloy matrix).

The normal load has the highest influence on wear, followed by the amount of graphite, the matrix material and the sliding speed, while the matrix material is the most influential factor on friction. The lowest wear rate was obtained for the composite based on A356 alloy, reinforced with 10 wt. % SiC and 1 wt. % Gr, at a normal load of 10 N and a sliding speed of 0.25 m/s. The lowest coefficient of friction was obtained for the composite based on ZA-27 alloy, reinforced only with 10 wt. % SiC, at a normal load of 10 N and a sliding speed of 1 m/s.

By examining the hardness of the produced composites for tribological tests, uniform results were obtained, which unequivocally confirms the good distribution of particles, as well as justification of application of this process for obtaining the composite materials. By adding the graphite, the coefficient of friction of the tested materials increased. The main reasons for that increase are the type of contact geometry, as well as a large drop in hardness of the tested material. A large decrease in hardness is evident in the composite with 3 wt.% Gr, where the coefficient of friction has the highest values.

Acknowledgements

This paper presents the research results obtained within realisation of the project TR 35021, supported by the Ministry of Science, Technological Development and Innovation of the Republic of Serbia. Aleksandar Vencl acknowledges the project financially supported by the Republic of Serbia, Ministry of Science, Technological Development and Innovation (Contract No. 451-03-47/2023-01/200105). Ruzica Nikolic acknowledges the project "Innovative Solutions for Propulsion, Power and Safety Components of Transport Vehicles", code ITMS 313011V334 of the Operational Program Integrated Infrastructure 2014-2020 co-financed by the European Regional Development Fund. Petr Svoboda acknowledges the project FSI-S-23-8245, funded by the Ministry of Education, Youth and Sports of the Czech Republic. Collaboration through the CEEPUS network CIII-BG-0703 and bilateral Project 337-00-577/2021-09/16 between Republic of Serbia and Republic of Austria is also acknowledged.

Conflicts of interest

The authors declare that they have no known competing financial interests or personal relationships that could have appeared to influence the work reported in this paper.

References

[1] OGUNDIJI, O. E., OYATOGUN G. M. Tensile and flexural properties of polyester composites reinforced by iron filings. *Tribology and Materials* [online]. 2022, **1**(4), p. 157-162. ISSN 2812-9717. Available from: https://doi.org/10.46793/tribomat.2022.020

[2] SARDAR, S., DEY, S., DAS, D. Modelling of tribological responses of composites using integrated ANN-GA technique. *Journal of Composite Materials* [online]. 2021, **55**(7), p. 873-896. ISSN 0021-9983. Available from: https://doi.org/10.1177/0021998320960520

[3] NWOBI-OKOYE, C. C., OCHIEZE, B. Q., OKIY, S. Multi-objective optimization and modelling of age hardening process using ANN, ANFIS and genetic algorithm: results from aluminum alloy A356/cow horn particulate composite. *Journal of Materials Research and Technology* [online]. 2019, **8**(3), p. 3054-3075. ISSN 2238-7854. Available from: https://doi.org/10.1016/j.jmrt.2019.01.031

[4] EKKA, K. K., CHAUHAN, S. R., GOEL, V. Study on the sliding wear behavior of hybrid aluminum matrix composites using Taguchi design and neural network. *Proceedings of the Institution of Mechanical Engineers, Part L: Journal of Materials: Design and Applications* [online]. 2016, **230**(2), p. 537-549. ISSN 1464-4207. Available from: https://doi.org/10.1177/1464420715581393

[5] GULER, O., CUVALCI, H., CANAKCI, A., CELEBI, M. The effect of nano graphite particle content on the wear behavior of ZA27 based hybrid composites. *Advanced Composites Letters* [online]. 2017, **26**(2), p. 30-36. ISSN 0963-6935, EISSN 2633-366X. Available from: https://doi.org/10.1177/096369351702600201

[6] CELEBI, M., GULER, O., CANAKCI, A., CUVALCI, H. The effect of nanoparticle content on the microstructure and mechanical properties of ZA27-Al2O3-Gr hybrid nanocomposites produced by powder metallurgy. *Journal of Composite Materials* [online]. 2021, **55**(24), p. 3395-3408. ISSN 0021-9983, eISSN 1530-793X. Available from: https//doi.org/z0.1177/00219983211015719

[7] GULER, O., CELEBI, M., DALMIS, R., CANAKCI, A., CUVALCI, H. Novel ZA27/B 4 C/graphite hybrid nanocomposite-bearing materials with enhanced wear and corrosion resistance. *Metallurgical and Materials Transactions A* [online]. 2020, **51**, p. 4632-4646. ISSN 1073-5615. Available from: https://doi.org/10.1007/s11661-020-05863-5

[8] FENG, C., WANG, Y., WANG, Z. Influence of graphite morphology on hyperthermal friction and wear behaviors of aluminum-high silicon alloys. *Silicon* [online]. 2022, **14**, p. 9153-9161. ISSN 1876-990X, eISSN 1876-9918. Available from: https://doi.org/10.1007/s12633-021-01524-3

[9] ASHEBIR, D. A., MENGESHA, G. A., SINHA, D. K., An insight into mechanical and metallurgical behavior of hybrid reinforced aluminum metal matrix composite. *Advances in Materials Science and Engineering* [online]. 2022, 7843981. ISSN 1687-8434, eISSN 1687-8442. Available from: https://doi.org/10.1155/2022/7843981

[10] BOBIC, I., RUZIC, J., BOBIC, B., BABIC, M., VENCL, A., MITROVIC, S. Microstructural characterization and artificial aging of compo-casted hybrid A356/SiC_p/Gr_p composites with graphite macroparticles. *Materials Science and Engineering A* [online]. 2014, **612**, p. 7-15. ISSN 0921-5093. Available from: https://doi.org/10.1016/j.msea.2014.06.028

[11] AJAY KUMAR, K., MALLIKARJUNA, C., Microstructure and mechanical properties of A356/Al_2O_3/MoS_2 hybrid nanocomposites. *Materials Today: Proceedings* [online]. 2022, **54**(2), p. 415-420. ISSN 2214-7853. Available from: https://doi.org/10.1016/j.matpr.2021.09.472

[12] VENCL, A., VUCETIC, F., BOBIC, B., PITEL, J., BOBIC, I. Tribological characterization in dry sliding conditions of compocasted hybrid A356/SiC_p/Gr_p composites with graphite macroparticles. *The International Journal of Advanced Manufacturing Technology* [online]. 2019, **100**(9-12), p. 2135-2146. ISSN 0268-3768. Available from: https://doi.org/10.46793/tribomat.2022.014

[13] GURUNAGENDRA, G. R., RAJU, B. R., PUJAR, V., AMITH, D. G., POORNACHANDRA, SIDDESHA, H. S., Mechanical, wear and corrosion properties of micro particulates reinforced ZA-27 hybrid MMC by stir casting: a review. *Materials Today: Proceedings* [online]. 2021, **46**(17), p. 7602-7607. ISSN 2214-7853. Available from: https://doi.org/10.1016/j.matpr.2021.01.892

[14] VENCL, A., STOJANOVIC, B., GOJKOVIC, R., KLANCNIK, S., CZIFRA, A., JAKIMOVSKA, K., HARNICAROVA, M. Enhancing of ZA-27 alloy wear characteristics by addition of small amount of SiC nanoparticles and its optimisation applying Taguchi method. *Tribology and Materials* [online]. 2022, **1**(3), p. 96-105. ISSN 2812-9717. Available from: https://doi.org/10.46793/tribomat.2022.014

[15] HAGHDADI, N., ZAREI-HANZAKI, A., KHALESIAN, A. R., ABEDI, A. R. Artificial neural network modelling to predict the hot deformation behavior of an A356 aluminum alloy. *Materials and Design* [online]. 2013, **49**, p. 386-391. ISSN 0261-3069. Available from: https://doi.org/10.1016/j.matdes.2012.12.082

[16] STALIN, B., KUMAR, P. R., RAVICHANDRAN, M., KUMAR, M. S., MEIGNANAMOORTHY, M. Optimization of wear parameters using Taguchi grey relational analysis and ANN-TLBO algorithm for silicon nitride filled AA6063 matrix composites. *Materials Research Express* [online]. 2019, **6**(10), 106590. eISSN 2053-1591. Available from: https://doi.org/10.1088/2053-1591/ab3d90

[17] DANIEL, S. A. A., PUGAZHENTHI, R., KUMAR, R., VIJAYANANTH, S. Multi objective prediction and optimization of control parameters in the milling of aluminum hybrid metal matrix composites using ANN and Taguchi-Grey relational analysis. *Defence Technology* [online]. 2019, **15**(4), p. 545-556. ISSN 2096-3459. Available from: https://doi.org/10.1016/j.dt.2019.01.001

[18] MILORADOVIC, N., VUJANAC, R., STOJANOVIC, B., PAVLOVIC, A. Dry sliding wear behavior of ZA27/SiC/Gr hybrid composites with Taguchi optimization. *Composite Structures* [online]. 2021, **264**, 113658. ISSN 1879-1085. Available from: https://doi.org/10.1016/j.compstruct.2021.113658

[19] STOJANOVIC, B., GAJEVIC, S., KOSTIC, N., MILADINOVIC, S., VENCL, A. Optimization of parameters that affect wear of A356/Al2O3 nanocomposites using RSM, ANN, GA and PSO methods. *Industrial Lubrication and Tribology* [online]. 2022, **74**(3), p. 350-359. ISSN 0036-8792 Available from: https://doi.org/10.1108/ILT-07-2021-0262

[20] STOJANOVIC, B., TOMOVIC, B., GAJEVIC, S., PETROVIC, J., MILADINOVIC, S. Tribological behavior of aluminum composites using Taguchi design and ANN. *Advanced Engineering Letters* [online]. 2022, **1**(1), p. 28-34. eISSN 2812-9709. Available from: https://doi.org/10.46793/adeletters.2022.1.1.5

[21] STOJANOVIC, B., BABIC, M., VELICKOVIC, S., BLAGOJEVIC, J. Tribological behavior of aluminum hybrid composites studied by application of factorial techniques. *Tribology Transactions* [online]. 2016, **59**(3), p. 522-529. eISSN 1547-397X. Available from: https://doi.org/10.1080/10402004.2015.1091535

[22] VORKAPIC, M., MLADENOVIC, I., PERGAL, M., IVANOV, T., BALTIC, M. Optimisation of tensile stress of poly(lactic acid) 3D printed materials using response surface methodology. *Tribology and Materials* [online]. 2022, **1**(2), p. 70-80. ISSN 2812-9717. Available from: https://doi.org/10.46793/tribomat.2022.009

[23] RAJESH, A. M., KALEEMULLA, K. M., SALEEMSAB D., BHARATH K. N. Generation of mechanically mixed layer during wear in hybrid aluminum MMC under as-cast and age hardened conditions. *SN Applied Sciences* [online]. 2019, **1**(8), 860. ISSN 2523-3971. Available from: https://doi.org/10.1007/s42452-019-0906-5

[24] SHETTY, R. J., HINDI, J., GURUMURTHY, B. M., HEGDE, A., SHIVAPRAKASH, Y. M., SHARMA, S., MURTHY, A., MURALISHWARA, K. Effect of metallic reinforcement and mechanically mixed layer on the tribological characteristics of Al-Zn-Mg alloy matrix composites under T6 treatment. *Cogent Engineering* [online]. 2023, **10**(1), 22009001. ISSN 2331-1916. Available from: https://doi.org/10.1080/23311916.2023.2200900